CHAPTER II

EXPERIMENTAL TECHNIQUES

The results described in the following chapters have been obtained using different experimental techniques, i.e., X-ray diffraction, high pressure and miscibility methods. The details of the apparatus used for the X-ray and high pressure studies form the subject matter of this chapter while those concerning miscibility techniques are discussed in Chapter V.

Two types of X-ray diffraction systems were used depending upon the requirement. For low resolution experiments and in particular where the complete picture in reciprocal space was necessary, the photographic technique was used. All the high resolution studies were carried out using a computer controlled Guinier diffractometer. We shall describe these two types of apparatus separately in the following sections.

2.1 X-RAY DIFFRACTION: PHOTOGRAPHIC TECHNIQUE

The schematic diagram of the set up is shown in Fig. 2.1. The experiments were performed using Cu-K_α radiation from a Philips X-ray generator (PW 1730). A quartz crystal monochromator (Carl-Zeiss Jena) was aligned to Bragg reflect the strongest K_a line. Two vertical slits S_1 and S_2 placed on either side

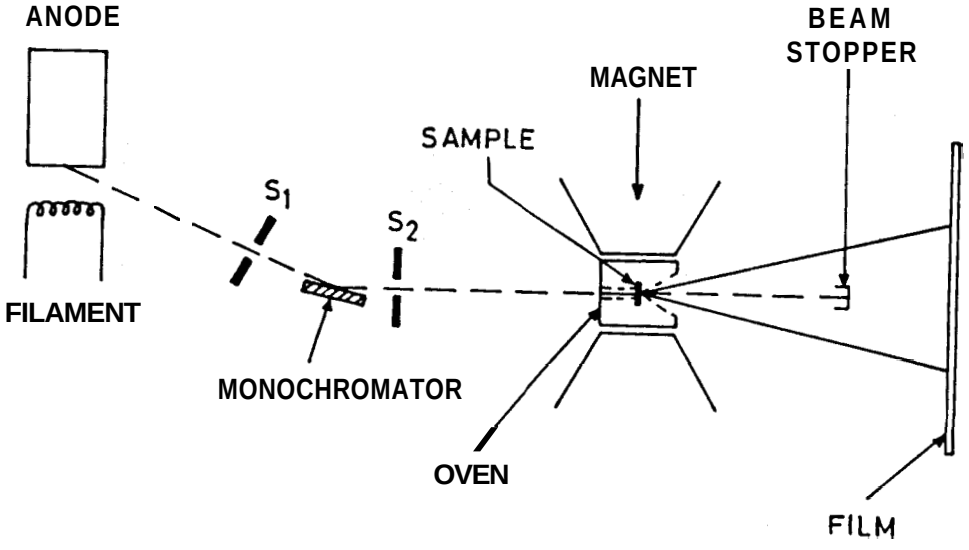

Figure 2.1

A schematic leplebentation of the scattering geometry.

of the monochromator (see Fig. 2.1) are narrowed down to eliminate further scattering from the tail ends of the nearby X-ray lines such as K_β and also to cut down the Bremsstrahlung background. X-rays after passing through the slit S_2 fall on the sample which is situated in a temperature controlled oven between the pole-pieces of a permanent magnet. The diffracted beam is recorded by a photographic film which is located at the focus of the monochromator. A regular 'beam stopper' was used to prevent the direct X-ray beam from striking the film. The details of the sample holder and the heater assembly are described in the following sections.

2.1.1 Sample Holder and Heater

Fig. 2.2 shows a schematic diagram of the sample holder and the heater assembly. The heater consisted of a rectangular copper block whose cross-section was chosen to facilitate an easy mounting between the pole-pieces of a permanent magnet. The copper block has a rectangular slot along its length which houses the sample holder. A tapered hole (O_1) was drilled at the centre of the heater (perpendicular to its long dimension) for X-rays to pass through. The tapered hole has a small diameter of 0.8 mm at the entrance side to collimate the X-ray beam. The side possessing the tapered hole is called as the exit side and the conical angle of the exit aperture was about 45°.

The sample holder (Fig. 2.2a) consisted of a long rectangu-

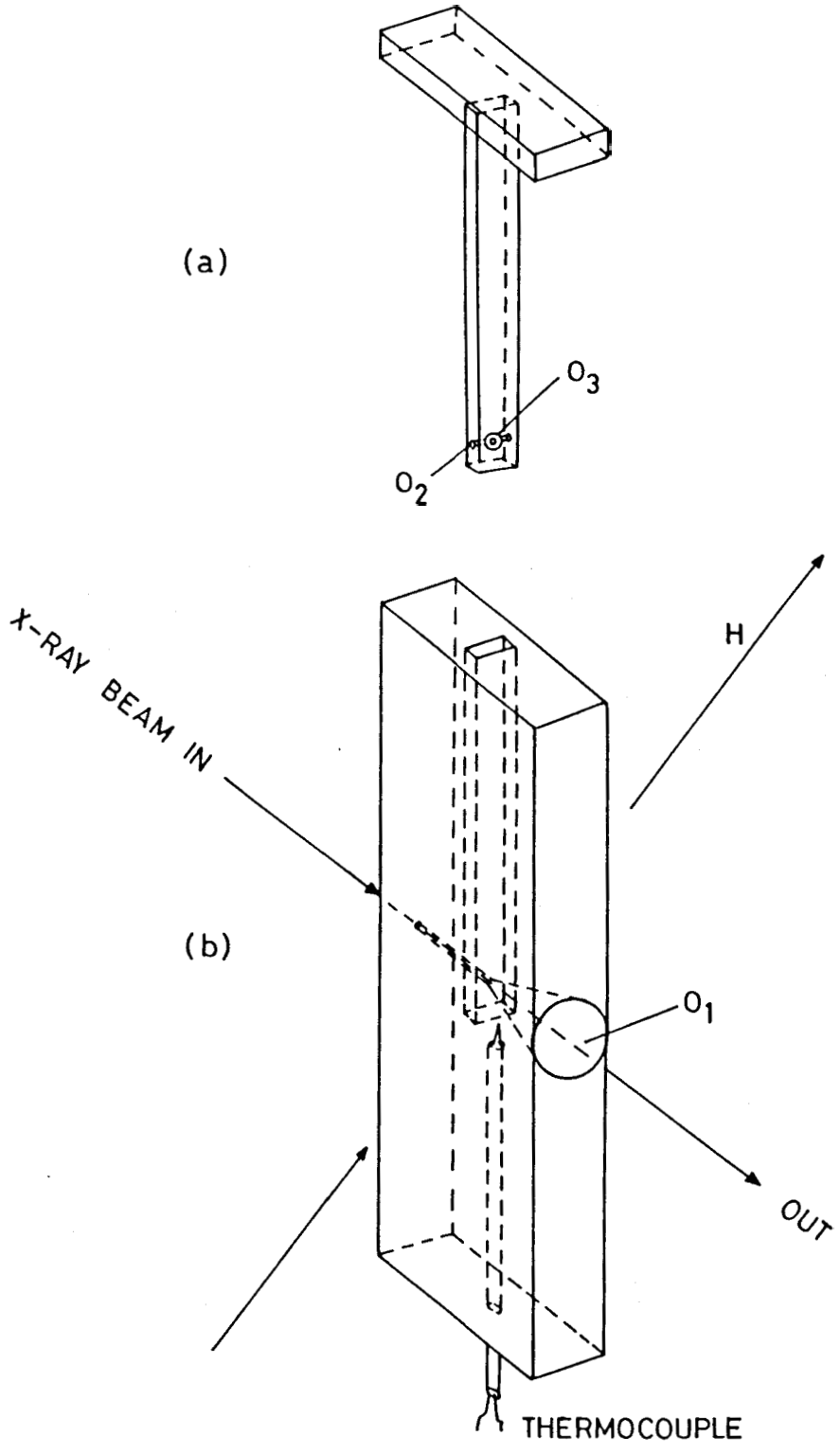

Figure 2.2. ***Schematic diagzam of the*** *(a)* ***oample*** *holder* ***and*** *(b) heater.* O_1 *- tapered* ***hole*** *for* ***the paooage*** *of Xrays,* O_2 *-* ***hole*** *for* ***the*** *insertion of the* ***Lindemann*** *capillary,* ***and*** O_3 *- hole for* ***the paooage*** *of Xrays.*

lar strip which fitted exactly into the rectangular slot of the holder. This enabled us to place the sample holder and hence the sample in the same position every time the sample was mounted. In this manner it was ensured that the sample-to-film distance was the same for every experiment. The sample holder has a hole (O_2) of 0.7 mm diameter along the wider side through which a Lindemann capillary containing the sample could be inserted. The sample holder has another hole (O_3) at right angles to the hole for the capillary and this hole matches the opening O_1 of the outer jacket of the heater. These set of openings collimate the X-rays to fall on the sample.

A hole drilled along the long dimension of the heater block from the bottom end houses one of the junctions of a chromel-alumel thermocouple sheathed in a ceramic tube. The ceramic tube was anchored to the heater block with an epoxy such that the thermocouple junction is located in close proximity of the sample. The heater assembly consisted of thermofoil (MINCO) wrapped around the copper block. These strips were covered by a thermally insulating material (hylam). A thin layer of asbestos paper separated the hylam from the thermofoil strips (see Fig. 2.3). This helped in minimizing the heat loss due to radiation. Thin mylar sheets (about 12 μm thick) were pasted on both sides of the tapered holes made on the hylam cover to prevent air currents and thereby avoiding fluctuations in the temperature of the sample. The temperature of the

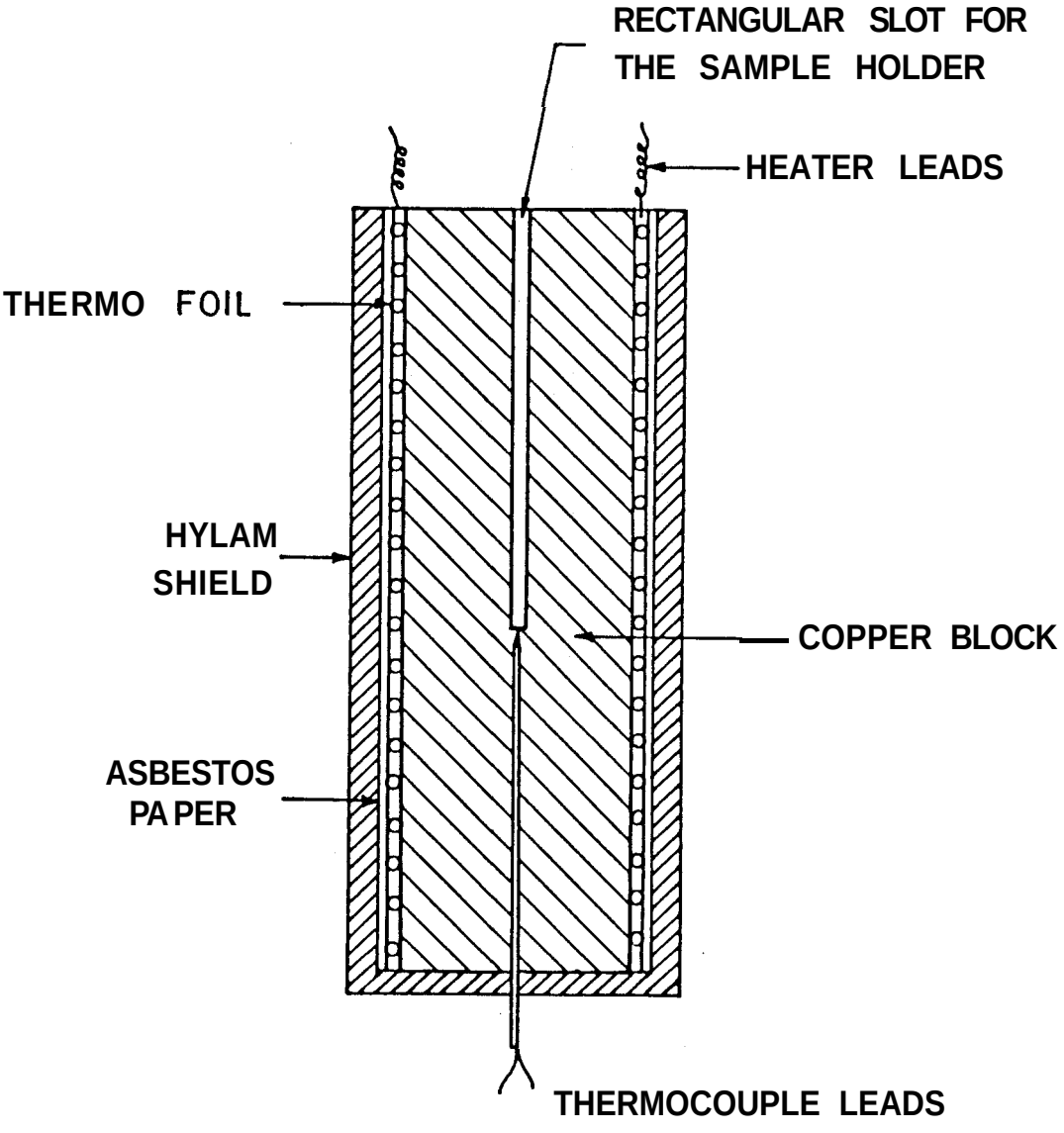

Figure 2.3

Cross-sectional view of the heatei along with the heatei assembly.

sample could be controlled by varying the current passing through the heater foil.

The heater assembly is placed between the pole-pieces of a permanent magnet (0.5 T) such that the sample is at the centre of the pole pieces and the field is normal to the incident X-ray beam. The heater and the magnet assembly are mounted on a stand whose height could be adjusted which in turn was fixed on a base consisting of three levelling screws. The electrical power to the heater was supplied by a highly stabilized D. C. power supply.

2.1.2 Temperature Calibration

Although the junction of the thermocouple was located very close to the sample in the capillary, the exact temperature of the sample is found to be different from that measured by the thermocouple. This 'gradient' depends on the experimental set up. It is necessary to determine this gradient very accurately over a wide range of temperature so that the 'true' sample temperature can be evaluated. This was achieved in the following manner.

Several compounds of high purity exhibiting sharp mesophase - isotropic or mesophase - mesophase transitions were chosen for temperature calibration. Samples were taken in Lindemann capillary tubes and the phase transitions were detected by the light transmission technique. Light from a He-Ne laser (Spectra Physics 120 S) was made to fall on the sample. The intensity of the laser light trans-

mitted by the sample was monitored by a photodiode. The output of the detector as well as the temperature were fed to two channels of a mutlichannel recorder. The temperature at which there was a sudden change in the transmitted light intensity was taken as the transition temperature (in mV). In this way the transition temperatures corresponding to the mesophase-isotropic and mesophase-mesophase transitions were determined both on heating and cooling modes. For the same materials these transition temperatures were determined using a polarizing microscope in conjunction with a programmable hot stage (FP82/FP800). The names of the compounds used in the calibration are listed in Table 2.1 along with the abbreviations used while their transition temperatures as determined in the heating and cooling modes are given in Tables 2.2 and 2.3 respectively. The transition temperatures (x in mV) as determined using the X-ray set-up are plotted versus the corresponding temperatures (in °C) determined using the Mettler hot stage and the plots are shown in Figs. 2.4 and 2.5 in the heating and cooling modes respectively. The data were then fitted to a second degree polynomial of the form $T = ax^2 + bx + c$ using a least square fit program and a HP86B computer. The values of the constants a, b, c are $-0.0644°C/mV^2$, $25.2517°C/mV$ and $1.3793°C$ respectively for the heating mode and $-0.0541°C/mV^2$, $25.1425°C/mV$ and $1.3713°C$ for the cooling mode.

2.1.3 X-ray Studies

The liquid crystal sample was filled into the Lindemann

Table 2.1

Materials used for the thermocouple calibration

Sl. No.	Compound	Abbreviation
1	4-n-Pentyl-4'-cyanobiphenyl	5CB
2	4-n-heptyl-4'-cyanobiphenyl	7CB
3	4-n-octyloxy-4'-cyanobiphenyl	8OCB
4	4-n-octyloxy-benzylidene-4'-cyanoaniline	8 . CN
5	4-cyanobenzylidene-4'-octyloxy-aniline	CBOOA
6	4,4'-di-n-heptyloxy-azoxybenzene	HOAB
7	4,4'-di-methoxyazoxybenzene (p-azoxyanisole)	PAA
8	4-hexyloxybenzylidenephenyl-azoxyanisole	6BPAA

Table 2.2

Thermocouple calibration of the heater during heating mode: . Materials used and their transition temperatures.

Sl. No.	Substance	Transition	Temp.(°C) by Mettler	Thermocouple reading(mV) by heater
1	5CB	Nematic - Isotropic	34.3	1.3075
2	7CB	Nematic - Isotropic	41.7	1.6025
3	8OCB	Smectic A -Nematic	67.15	2.625
		Nematic - Isotropic	80.6	3.165
4	8S5	Nematic - Isotropic	99.05	3.880
5	CBOOA	Smectic A - Nematic	82.9	3.2525
		Nematic - Isotropic	107.9	4.275
6	HOAB	Smectic C-Nematic	95.55	3.725
		Nematic - Isotropic	124.6	4.9675
7	PAA	Nematic - Isotropic	135.9	5.4
8	6BPAA	Nematic - Isotropic	173.75	6.950

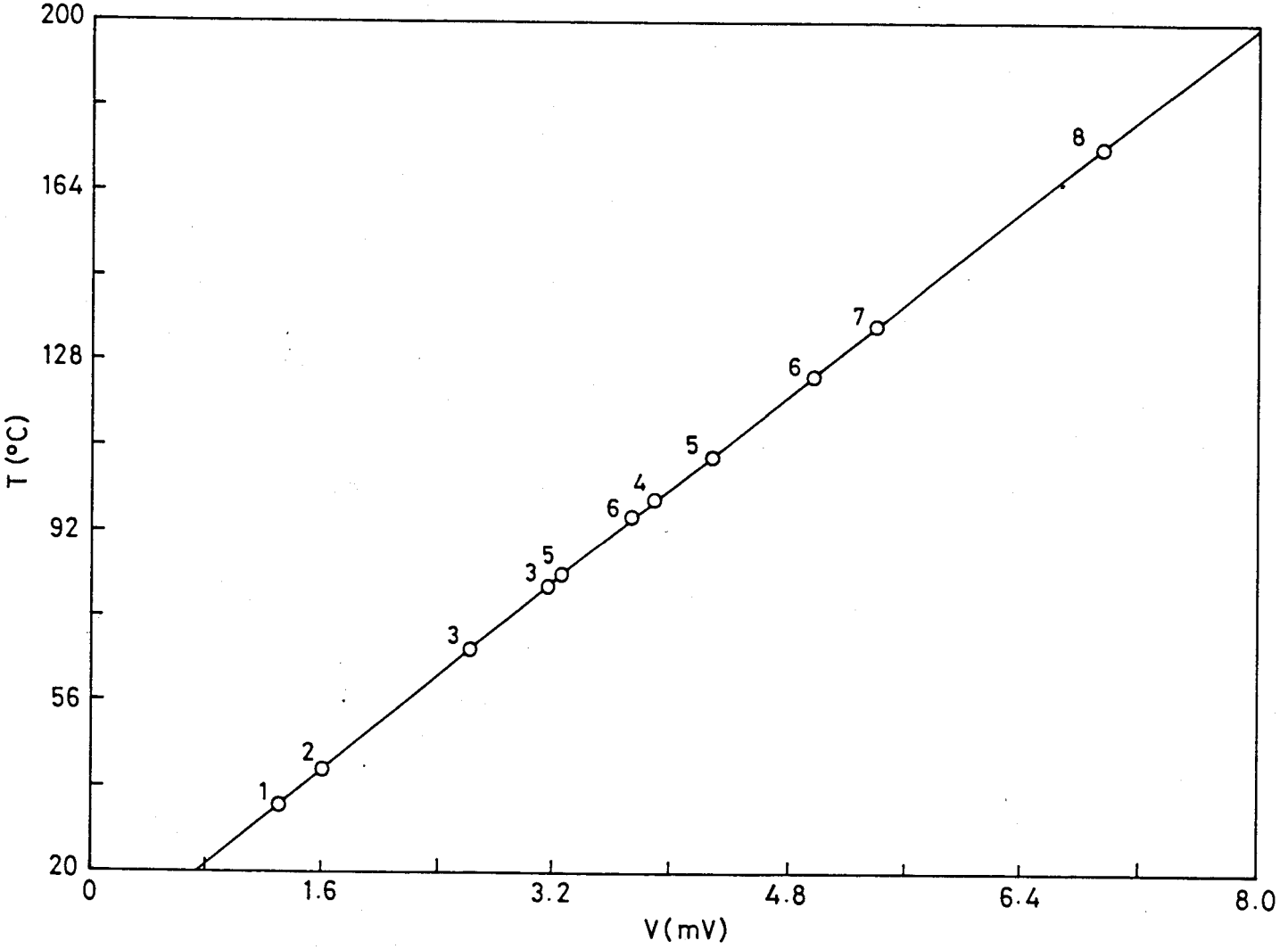

Figure 2.4. Temperature calibration curve of the Xray heater in the heating mode. The data points 1,2,3,....., are for substances listed in Table 2.2.

Table 2.3

Thermocouple calibration of the heater during cooling mode: Materials used and their transition temperatures.

Sl. No.	Substance	Transition	Temp. (°C) by Mettler	Thermocouple reading (mV) by heater
1	5CB	Isotropic - Nematic	33.90	1.2975
2	7CB	Isotropic –Nematic	41.40	1.595
3	8OCB	Isotropic– Nematic	80.25	3.1575
		Nematic - Smectic A	66.85	2.620
4	$\bar{8}$. CN	Isotropic–Nematic	98.60	3.880
5	CBOOA	Isotropic - Nematic	107.60	4.2725
		Nematic - Smectic A	82.50	3.2525
6	HOAB	Isotropic –Nematic	124.40	4.9675
		Nematic - Smectic C	95.05	3.730
7	PAA	Isotropic –Nematic	135.60	5.395
8	6BPAA	Isotropic –Nematic	173.40	6.945

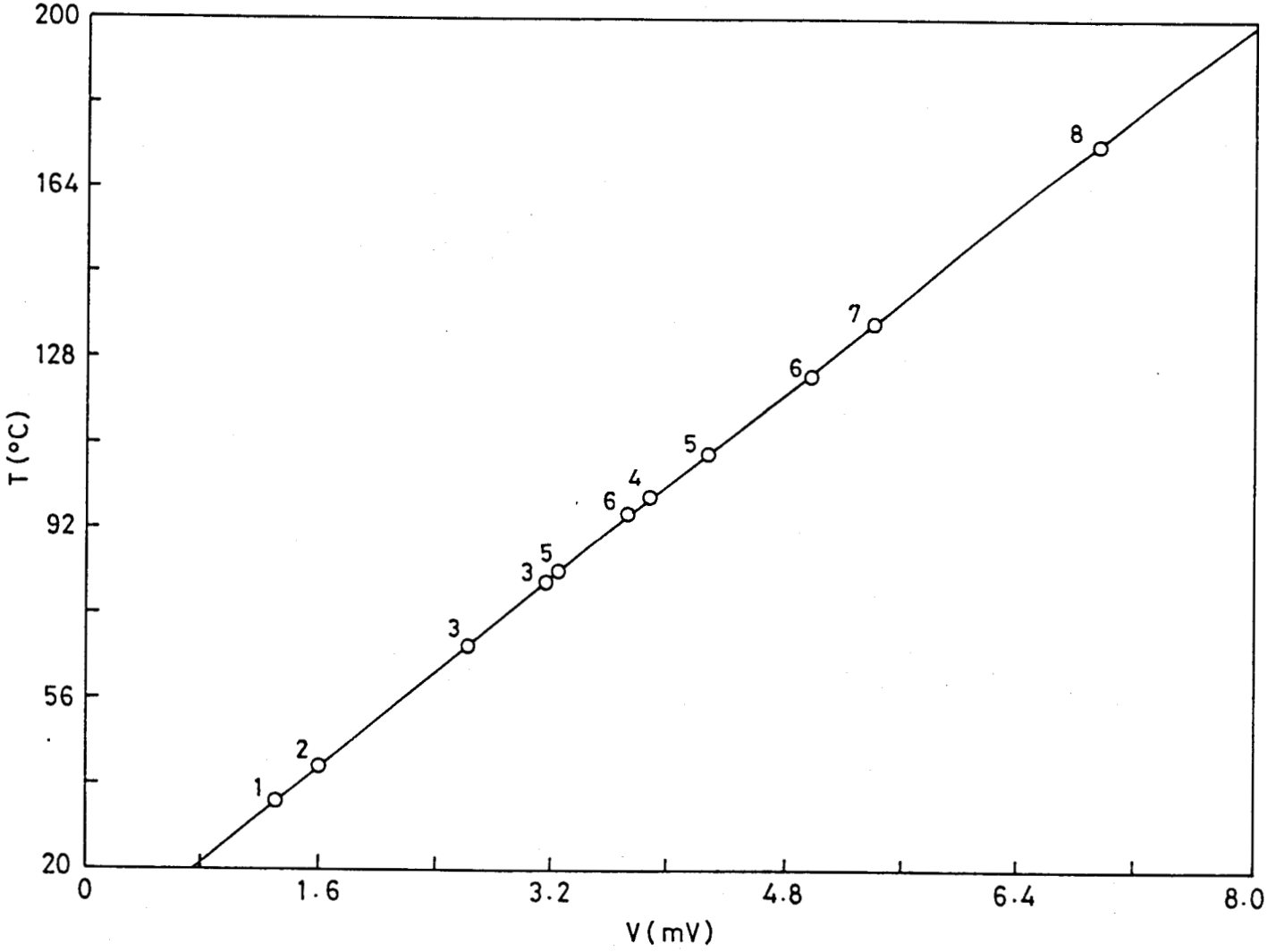

Figure 2.5. Temperature calibration curve in the cooling mode. The data pointb marked 1, 2, ..., referred to the substances listed in Table 2.3.

capillary tube in the molten state by means of a microsyringe. After filling the sample, the ends of the tubes were sealed using a thin flame. Care was taken to see that sample remains quite far from the sealed ends. The capillary tube with the sample was then loaded into the sample holder. The sample was heated to the nematic phase and slowly cooled in the presence of a magnetic field of strength 5 Kgauss to get an oriented sample and was then irradiated with monochromatic CuK_{α} radiation. The diffracted X-ray beam was recorded on a flat photographic film kept at a distance of approximately 15 cm from the sample. Depending on the sample, the exposure time varied from 10-15 minutes. After the completion of the experiment, the transition temperatures of the sample was remeasured and was found to be (within the limits of experimental error) the same as those before commencement of the experiment. Thus it was ascertained that the sample did not deteriorate during the exposure time. The sample to film distance was standardized by using the (100) reflection of p-decanoic acid, the d-value of this reflection being taken to be 23.1 . The distance between the diffraction spots on the film was measured using an accurate comparator (Adam-Hilger). The accuracy of layer spacing measurement is found to be ± 0.1 Å.

2.2 X-RAY DIFFRACTION: COMPUTER CONTROLLED GUINIER DIFFRACTOMETER

A schematic view of the scattering geometry used in the experiments conducted using the Guinier diffractometer (Huber 644)

is shown in Fig. 2.6.

2.2.1 Source and Detector

A conventional X-ray generator (Enraf Nonius 583) with a fine focus tube with a copper target was used. The power used was about 1.3 Kwatt (50 KV and 26 mA). The beam from the X-ray tube enters the monochromator after passing through a short vacuum flight path. The monochromator input slits were kept wide open to avoid spurious trimming of the incoming beam. By using a bent quartz crystal monochromator cut for $(10\bar{1}1)$ reflection in the Johansson geometry, it was possible to separate the $K_{\alpha 1}$ and $K_{\alpha 2}$ lines. Only the K_{a1} line was used for the experiments. These $K_{\alpha 1}$ Xrays get focussed at a point on the circumference of the Guinier circle. The detector (i.e., NaI scintillation counter, Bicron) was mounted on the arm (of the diffractometer) which moves along the c'ircumference of the Guinier circle for asymmetric transmission mode. A platinum edged slit, which was razor sharp to eliminate any shadow effects was used to collimate the beam falling on the counter. To get a good vertical collimation of the scattered beam, a pair of soller slits were positioned in front of the detector. The arm holding the detector was driven by a stepper-motor with an angular resolution of 0.001 of a degree. The beam stopper positioned in between the sample and the detector prevented the direct beam from hitting the detector.

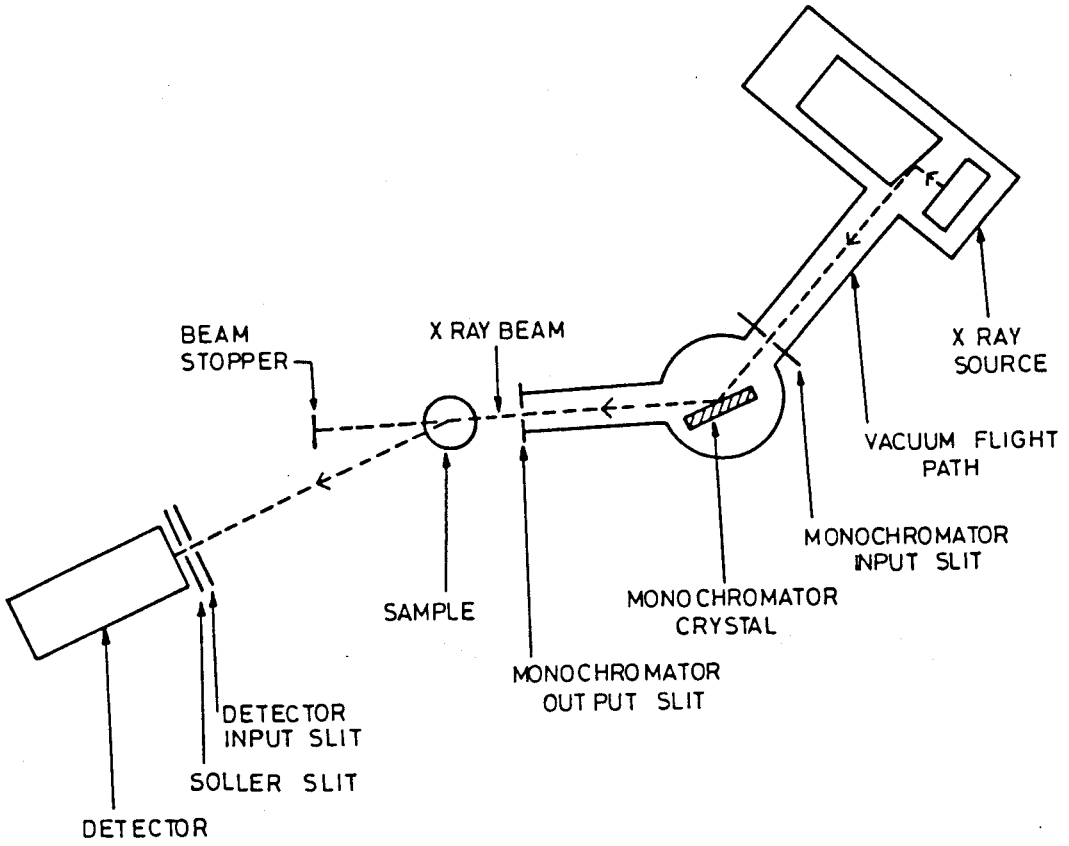

Figure 2.6. Schematic diagram of the Xray diffraction set up.

2.2.2 Sample Holder and Heater Design

A schematic representation of the sample holder is shown in Fig. 2.7. It consists of a copper rod in which a narrow bore (0.7 mm diameter, 15 cm length) was drilled along its vertical axis from the top end so as to hold the Lindemann capillary containing the liquid crystal sample. A pair of slots are cut on the rod along the length and diametrically opposite to each other. These slots serve as the entrance and exit slits for the X-ray beam. Also, the edges of the exit slit are tapered so as to have a conical angle of about 30°. The stem at the lower end helps in fixing the sample holder on the goniometer base.

A sectional view of the heater (oven) used to heat or cool the liquid crystal samples is given in Fig. 2.8. It consists of a thick copper rod which has a cavity cut along the cylindrical axis to accommodate the sample holder. The dimensions of the sample cavity are so chosen that the sample holder fits exactly into it. Two vertical slots are cut on the cylinder, one on either side, to serve as the entrance and exit slits (windows) for the X-ray beam. A hole, drilled from the top of the heater along the axis of the copper rod, houses a chromel-alumel thermocouple sheathed in a ceramic tube. The junction of the thermocouple was positioned with an adhesive so that it sits in close proximity of the sample. The temperature of the sample was varied by regulating the current passing through thermofoil (MINCO) strips wrapped around the copper

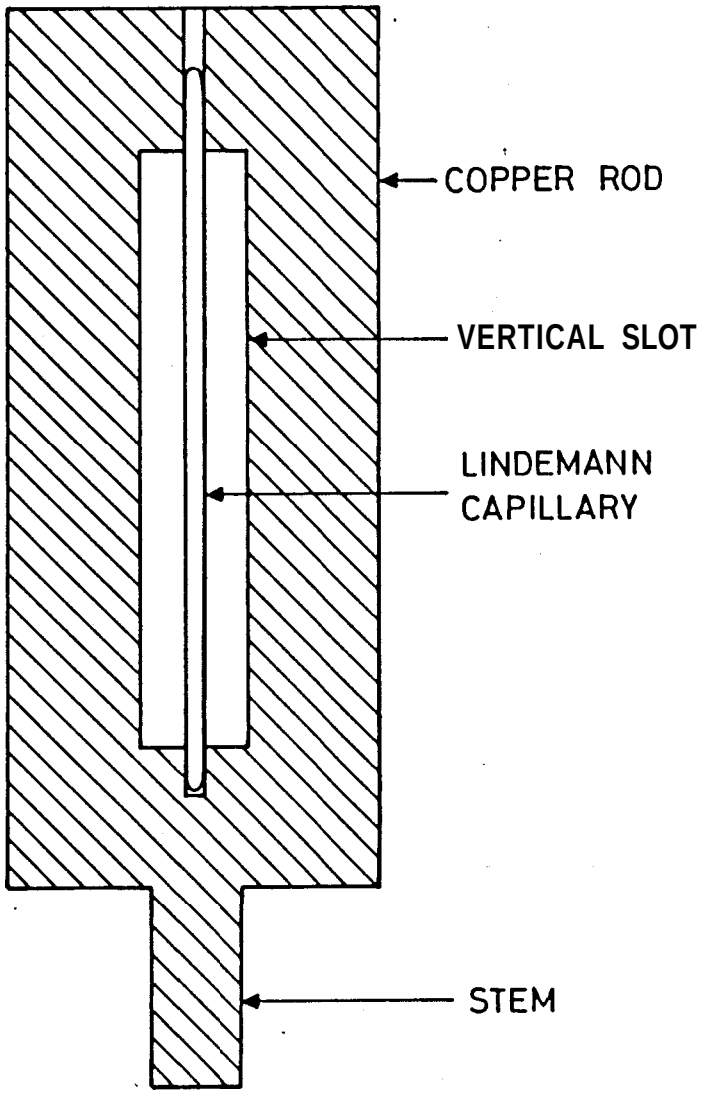

Figure 2.7

A cross-sectional view of the sample holder.

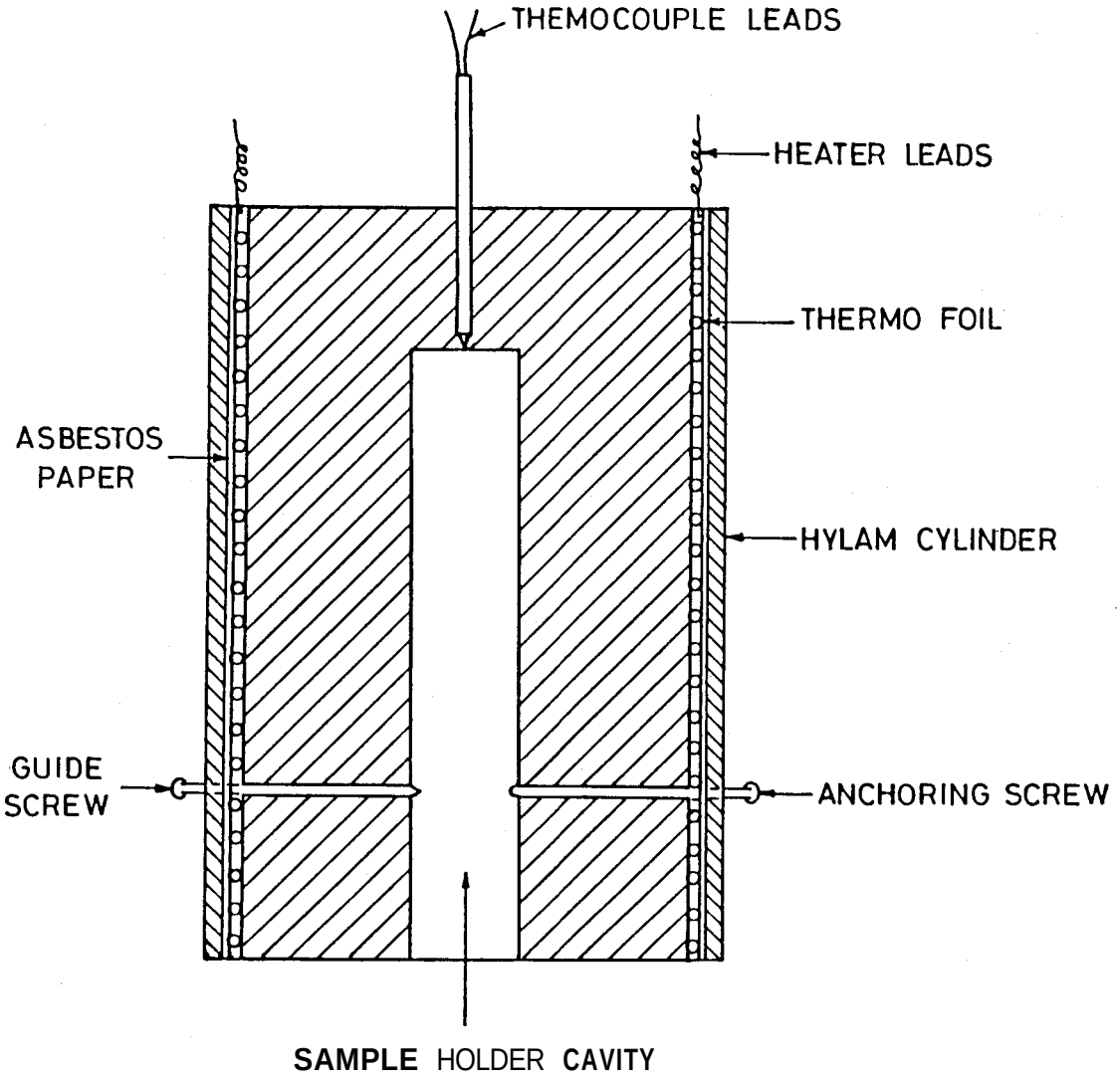

Figure 2.8

A cross-sectional view of the heater assembly.

rod. To minimize the heat loss due to radiation it was necessary to cover the heater assembly by means of a thermally insulating (hylam) cylinder. This material was separated from the thermofoil strips by means of a thin sheet of asbestos paper. A thin mylar sheet (12 μm thick) served to cover both sides of the windows on the cylinder in order to prevent air currents. A guiding screw threading through the body of the heater helps in ensuring that the sample holder can be inserted into the heater only in one position. For this purpose, a matching groove was made along the axis of the sample holder which was anchored to the heater by means of a screw located diametrically opposite to the guiding screw. These two screws are also used for anchoring the hylam cylinder to the heater body. Thus it was made sure .that the exit side of the sample holder always matches the exit side of the heater. The material of the heater and the sample holder as well as their dimensions are so chosen that there is no vertical temperature gradient along the length of the sample. Also, the temperature of sample could be maintained to within ± 10 mK during any measurement. To increase the efficiency in controlling and maintaining the sample temperature, the whole sample assembly was fully enclosed inside a good thermally insulating chamber.

The temperature of the sample was probed using a chromel-alumel thermocouple whose output was fed to a digital nanovoltmeter (Keithley 181). The thermocouple was calibrated in the manner descri-

bed in Section2.1.2 so as to give the correct temperature of the sample.

2.2.3. **Measuring Electronics and Data Collection**

A block diagram of the diffractometer set up is shown in Fig. 2.9. The working of the diffractometer was controlled by a computer (Hewlett Packard, 86B) with 128 kbytes of physical memory. All the instruments were interfaced to the computer by serial/ parallel Interface Bus. The detection electronics consists of the detector, a pulse height analyser and high voltage power supplies. Pulses from the detector after being fed through the amplifier and the discriminator reach the ratemeter where the intensity of the X-ray beam is expressed as counts per second. The discriminator output is fed to a stepper motor control. The data collection is done by means of an elaborate program which controls counting, duration of counting time, driving of stepper motor, data storage and data analysis. We shall describe in the following a typical experiment carried out using this set-up.

2.2.4 A Typical Experiment

The liquid crystal sample was filled in a Lindemann-capillary as described in Section 2.1.1(d). The sample was initially heated to the nematic phase and then cooled slowly into the smectic A in presence of a strong magnetic field (2.4 Tesla) using a Bruker electromagnet (B.E-25) with tapered cobalt-iron pole-pieces. This

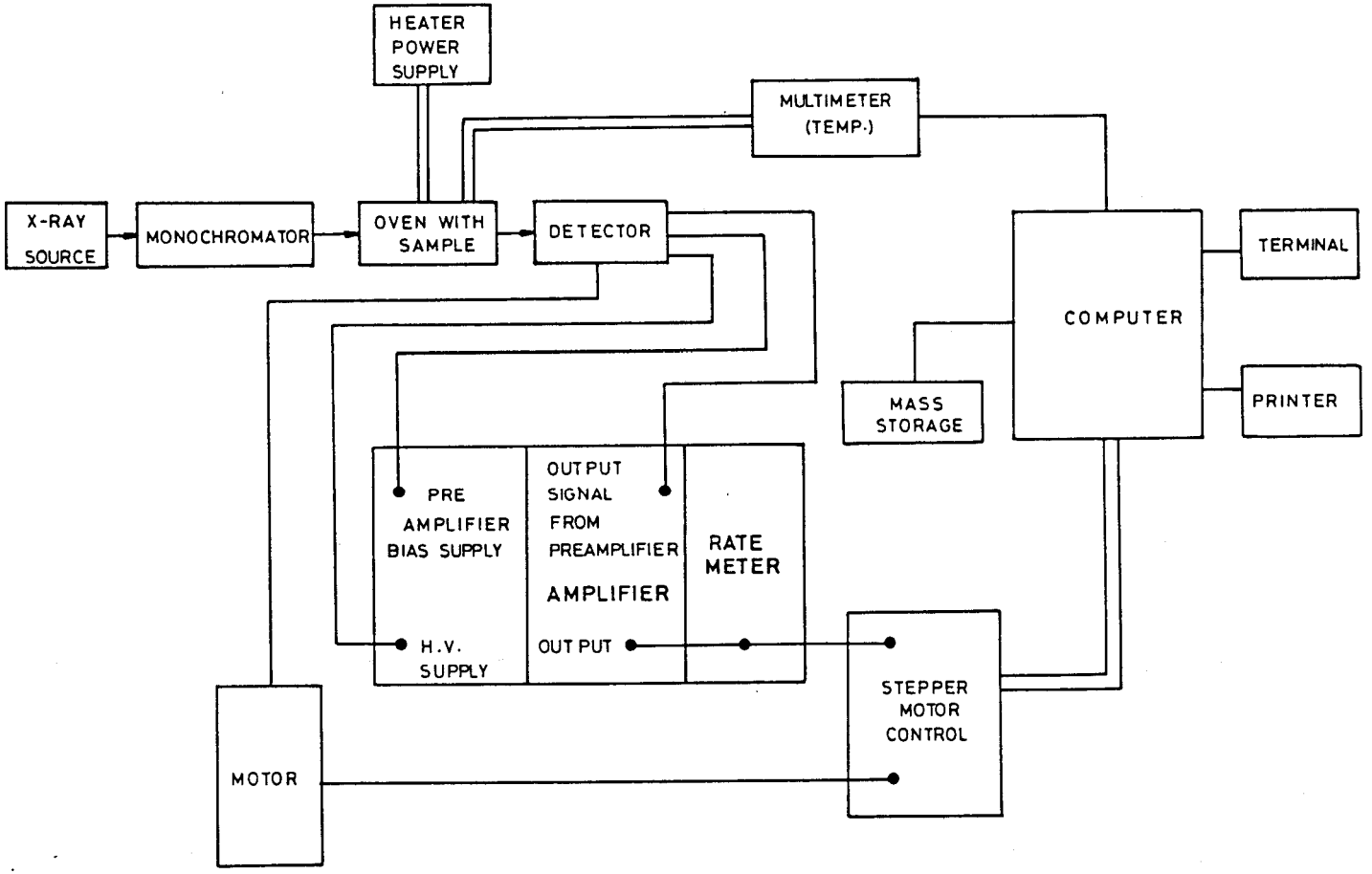

Figure 2.9

Block diagram of the diffraction set up.

resulted in a very well aligned A phase. The oriented sample (in the A phase) was then transferred along with the temperature controlled oven onto the goniometer base. An initial scan was taken by changing the position of the counter in steps of 0.01° and the approximate position (θ) of the diffraction peak was obtained. A refined θ scan was then taken around this θ position by moving the counter in steps of 0.001 of a degree. The data were fitted to a second degree polynomial by using a least-square-fit program. The value of θ obtained in this way was corrected, as it is possible that the layer spacing determined in the manner described above may differ from the expected values because of the limitations imposed by the experimental conditions. A calibration was carried out by measuring the layer spacing for a series of materials for which accurate layer spacing data is available.[2,3] By comparing the measured and the literature values, the correction to the measured θ was determined using the standard interpolation technique. Using the corrected θ, the layer spacing was determined from the relation $d = \lambda/2\sin\theta$. The on-line θ-refinement of a peak at any temperature required 2 minutes. During this period the temperature of the sample was maintained to a constancy of better than ± 10 mK.

2.2.5 Wavevector Resolution

The line shape observed in an X-ray scattering experiment is given by the convolution of the structure factor and the spectro-

meter resolution function. The latter includes broadening of the peak due to slit width, sample size and the Darwin width of the monochromator crystal. In our experiments the resolution of the instrument is also influenced very much by the sample mosaicity. Even at the smallest slit width permitted by the set up (10 μm) an I-θ scan (intensity - scattering angle) shows a peak with half width at half maximum of 0.01°.

The wavevector spread (dq) in the equatorial direction due to this angular width $d\theta \sim 0.01°$ as calculated from the equation

$$dq = \frac{4\pi}{\lambda} \cos\theta \, d\theta$$

for a typical scattering angle of $-0.88°$ is $dq = 1.42 \times 10^{-3}$ $\mathring{A}^{-1}$. In other words this set up permits us to resolve two peaks whose minimum separation in q space is 1.4×10^{-3} $\mathring{A}^{-1}$. The precision in the determination of q itself at any temperature is $\pm 2 \times 10^{-4}$ $\mathring{A}^{-1}$.

2.3 HIGH PRESSURE OPTICAL CELL

A variety of high pressure cells have been used so far[4-9] to study phase transitions in liquid crystals under high pressure. Amongst these the most successful has been the optical high pressure cell which is a direct-pressure transmitting cell. Such a cell already existed in the laboratory and has been used for extensive studies on liquid crystals.[4,8-10] A few modifications are

made to this cell for the following reasons : -

(i) the cell has to be capable of both microscopic and light scattering studies, and

(ii) it has to work even for very small quantities of materials (5 mg or even less). A description of the cell is given below.

2.3.1 Description of the Cell

A schematic diagram of the high pressure optical cell is given in Fig. 2.10. All the components of the cell are machined out of a low alloy hardenable steel, viz., EN-24 (equivalent to AISI 4130) which has 0.4% carbon, 0.2% silicon and 0.55% nickel. This steel has the advantage that it can be hardened to great strengths by means of martensitic transformation. The alloying elements increase hardenability of the material and in addition, also contribute with solid-solution strengthening. The different parts of the cell were machined and heat treated to hardness ranging from 40 to 55 RC depending on the component and its location in the cell.

The body of the cell (Fig. 2.11) has threaded openingson both sides into which two plugs (see Fig.2.10) with exactly matching threads can be fitted. On the outside, the plugs have a large tapered opening (70° outside taper) which facilitates a wide viewing angle without affecting the strength of the plug. On the inside, the plugs have a small protrusion which is made optically flat by hand-lapping. These plugs keep the sample assembly in position.

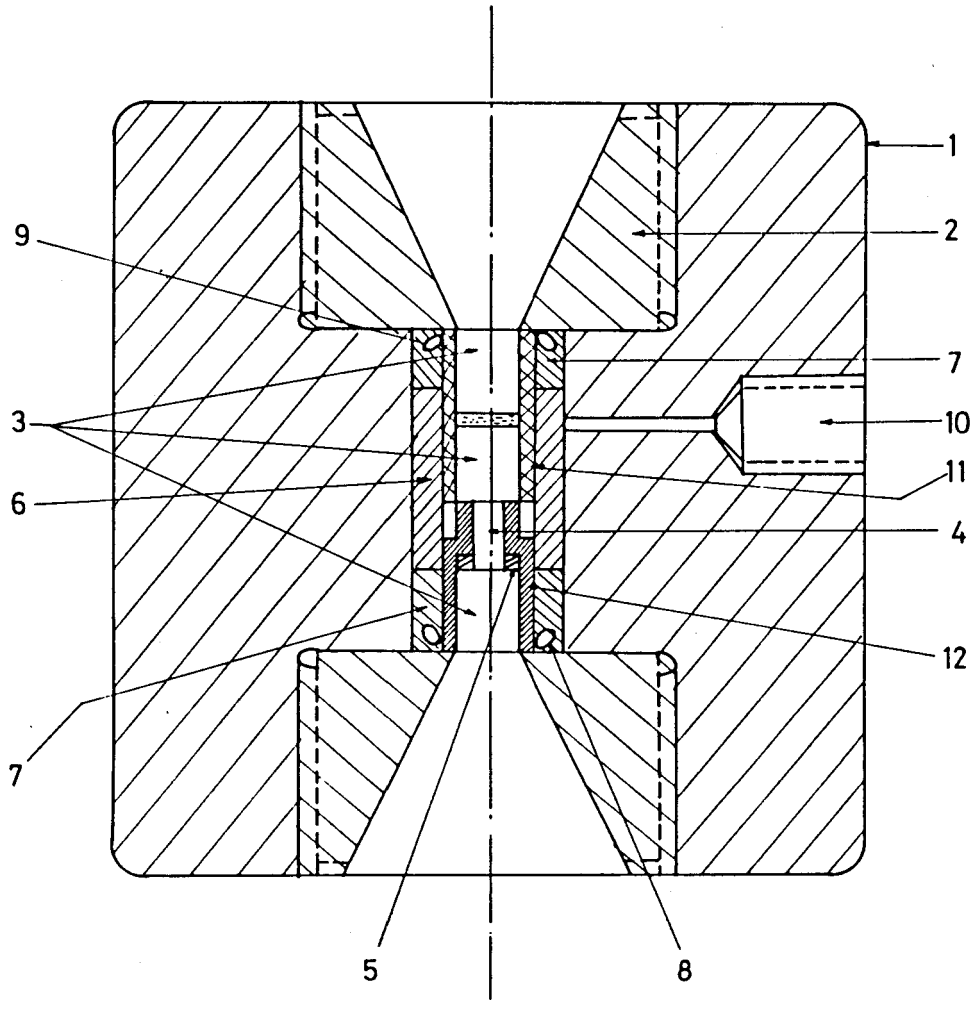

1. CELL BODY 2. STEEL PLUG 3. SAPPHIRE CYLINDERS
4. GLASS ROD 5. WASHER AND SPRING 6. CENTRE SPACER
7. OUTER SPACER 8. 'O' RING 9. ANTIEXTRUSION RING
10. HIGH PRESSURE CONNECTION 11. FLURAN TUBE 12. LOW-PRESSURE SEALER

FIG.2.10. HIGH PRESSURE OPTICAL CELL

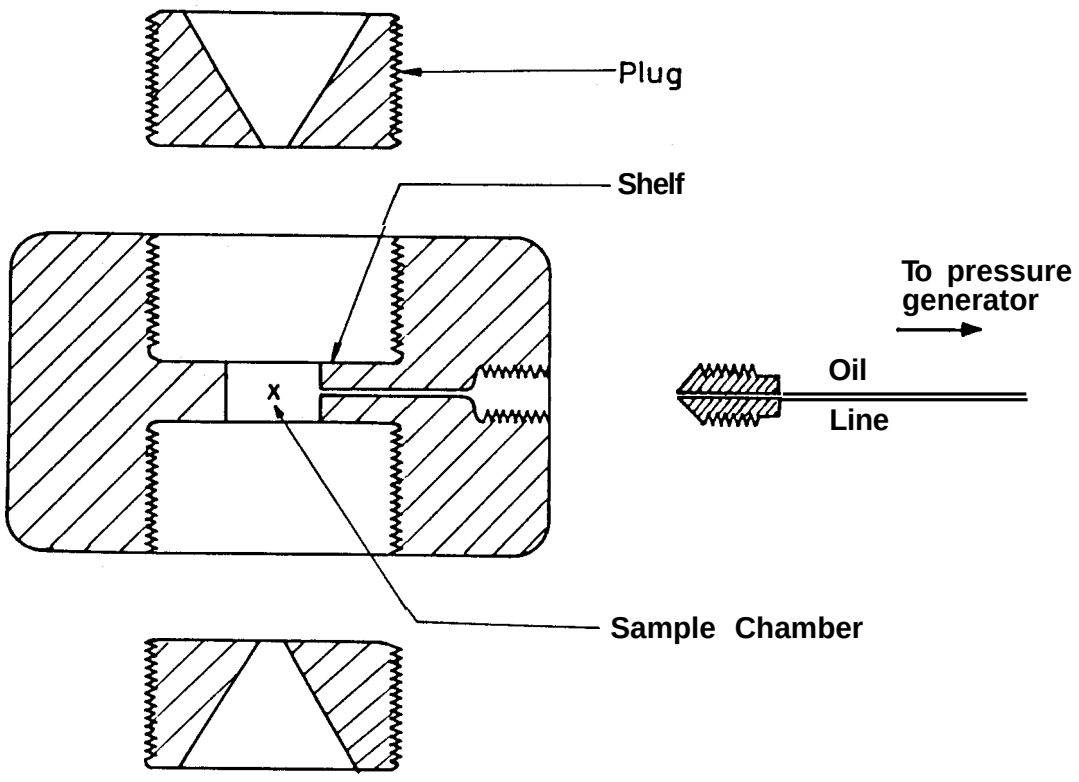

Figure 2.1 1. Schematic representation of the basic parts of the high pressure cell.

The central hole of the upper plug is sealed by an optically polished sapphire rod which also forms a part of the sample assembly. The hole in the cell body for the pressure connection consists of two stages: a smaller hole which extends from the interior of the body to about two-thirds of the thickness and joins a larger hole bored from outside.

2.3.2 Sample Chamber

In order to develop high pressure in the small central sample chamber, it is essential to have a tight seal along both boundries of the plugs: one for the central hole and the other along the circular boundary of the chamber against the plug. The reason for the latter is that the threads of the plug alone are not enough to hold the plug tightly against the main body of the cell. A thin clearance between the plug and the sample chamber caused by a slight lifting of the plug by high pressure leads to a leak of the oil to the outside. This leak is avoided by placing around the junction a neoprene 'O' ring in conjunction with an anti-extrusion ring. The seal at the central hole of the plug is made with optically polished sapphire windows and a small washer made of thin aluminium foil - the washer fills any crevices on the surface of the plug. The sapphire windows as well as the 'O' ring are held in position initially by the outer spacer.

2.3.3 Encapsulation of the Sample

It is well known that liquid crystals interact with pressure

transmitting media - gas or liquid. It is therefore necessry to isolate the sample from the pressure transmitting medium.This is achieved by using a fluran tubing. Fluran, an elastomer material does not react with liquid crystals and at the same time transmits pressure exceedingly well. It can also withstand temperatures up to about 270°C. The sample assembly is schematically represented in Fig. 2.12. The sample sandwiched between two sapphire rods which fit snugly inside the fluran tube. An effective seal is realised by tightly wrapping a thin steel wire around the tubing on the sapphire windows. The inner spacer (low pressure sealer), washer and the spring (see Fig. 2.10) centre the bottom sapphire (which is free as it is not used to seal the cap) of the sample assembly and keep it under a high tension. The third sapphire which is completely isolated from the sample assembly seals the bottom end of the pressure cell. The space between this third sapphire and the bottom sapphire of the sample assembly is occupied by a glass rod reducing thereby the amount of oil between these two sapphires which otherwise would have decreased the intensity of the transmitted light. It must also be mentioned that all three sapphire rods are specially cut such that the c-axis is perpendicular to the faces.

2.3.4 Description of the Heating and Cooling Systems

Most of the experiments conducted by us required quite high temperatures (about 200°C) and hence it was necessary to have

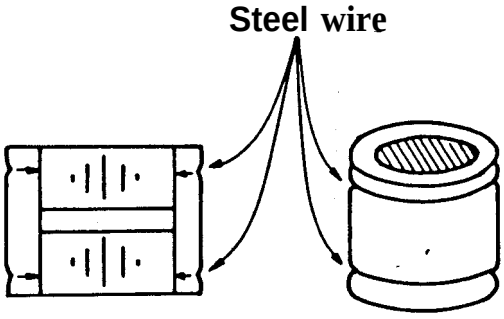

Figure 2.12. Sample Assembly

a heating system which can raise the temperature of the entire pressure cell to these relatively high temperatures. Fig. 2.13 shows the schematic diagram of the heater and cooler assemblies. The heating system is made of an aluminium cylinder whose internal diameter is such that the pressure cell would be push-fitted into it. Thus it also acts as a binding ring for the pressure cell. Nichrome tape was wound on mica sheets which in turn were wrapped around the inside wall of the aluminium cylinder. The effective heating capacity was about 200 watts. A radial hole was made through the aluminium cylinder to facilitate the taking out of the pressure tubings from the pressure cell to the outside. A chromel-alumel thermocouple sheathed in a ceramic tube was used to measure the temperature sensed by the sample. The thermocouple is introduced through a small radial hole and is so located that its junction just touches the cell body. No holes are made on the cell body for the insertion of the thermocouple since that would considerably weaken the cell body. There will be however a difference in the temperature of the sample and that sensed by the thermocouple junction. By accurately mapping this gradient at all temperatures, this problem was overcome. These calibration experiments were performed using a uniform heating or cooling rate of 1°C/min.

A cooling unit was used only when the cell had to be cooled to sub-ambient temperatures. Above room temperature cooling could be done by merely varying the current through the heating element.

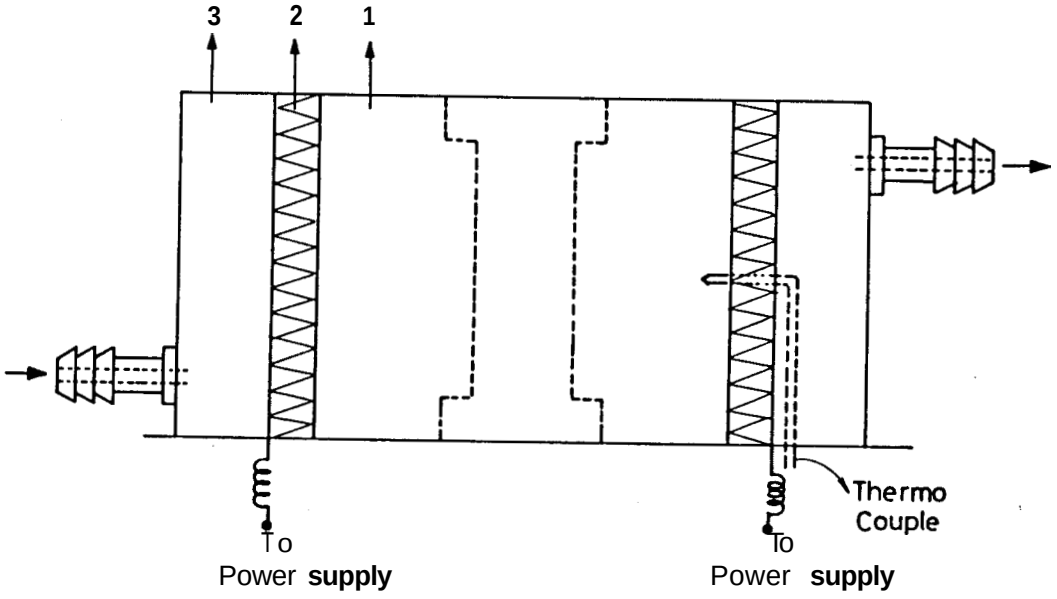

Figure 2.13

Schematic diagram of the heating and coofing assembly.

1. ***High Pressure Cell***
2. *Heater*
3. *Cooling* ***Unit*** .

A cooling jacket is made using aluminium as the material into which the cell can be press-fitted. By suitably scooping out the inside material from the jacket and by closing the top of the jacket with an aluminium strip, water can be passed into the jacket through the nozzles provided at the ends of the jacket. In fact, the jacket consisted of two 'c' shaped units linked by a hinge. So whenever cooling was necessary it could be slipped through easily. A thermostat was used to pump water into the cooling jacket. The water, as it passes through the entire circumference of the cooling jacket, provides a very efficient way of cooling the cell.

2.3.5. High Pressure Plumbing System

The schematic diagram of the high pressure plumbing system is shown in Fig. 2.14. A hand-pump (PPI, USA) is used to generate the pressure in the cell. Fine variations of pressure are achieved by using a pressure generator (HIP, USA) with a small displacement capacity. The line pressure, which is nothing but the pressure experienced by the sample, is measured by a Bourdon type (HEISE) gauge. The plumbing connections are made through two-way and three-way valves. The advantage of using a three-way valve over that of a T-joint is that the instrument which is connected through the valve can be isolated from the mainline when not in use by just closing the valve. Thus, for example, a pressure transducer could be used "on-line" whenever required. The tubing used was made of

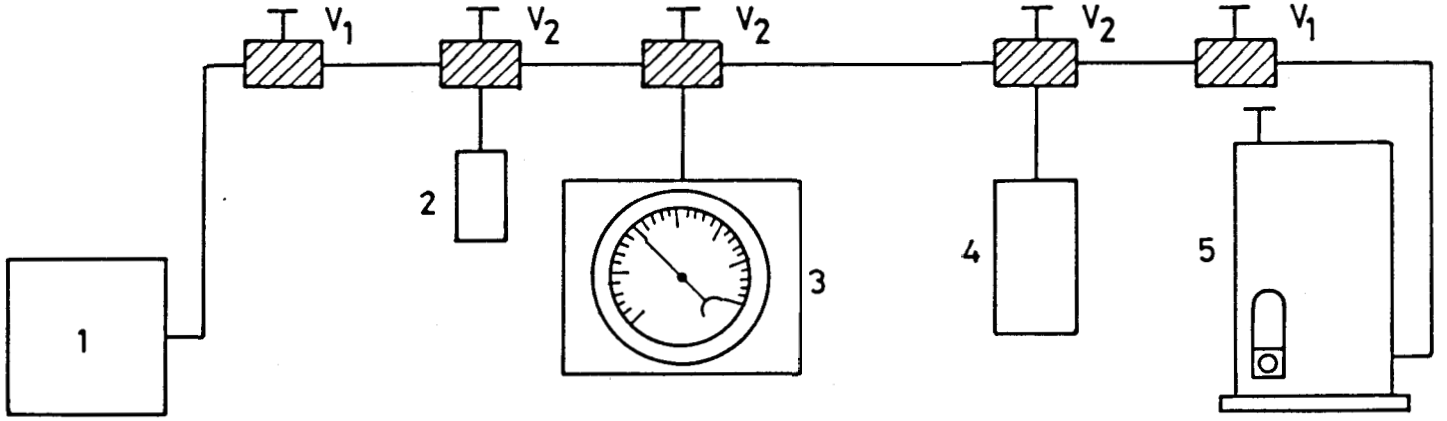

Figure 2.14

Schematic diagram of the high pressure plumbing system.

1. *High pressure cell*
2. *Pressure transducer*
3. *Bourdon gauge*
4. *Pressure generator*
5. *Hand pump.*

V_1. *Two-way valve*

V_2. *Three-way valve*

seamless stainless steel material (ID = 2 mm and OD - 10 mm). The valves as well as the tubing were chosen to withstand line pressures up to 7 kbar.

The sample was pressurised in a fairly straightforward way: the "priming" was done using the hand-pump. Pulling the handle of the pump up raises the piston and draws oil from the reserve into the pump's chamber. Pushing the handle down lowers the piston which compresses the oil and sends it through the steel line into the cell. After this priming operation pressure could be fine controlled using the pressure generator. As the pressure in the cell is the same as that in the pump the cell pressure could be indirectly measured by measuring the line pressure.

2.3.6. Determination of the Phase Transition Temperature by Optical Transmission Technique

The schematic diagram of the optical transmission technique is shown in Fig. 2.15. The transition temperatures were determined as discussed in Section 2.1.2.

2.3.7 Temperature Calibration of the High Pressure Cell

For an accurate temperature calibration of the high pressure cell during heating and cooling modes, several compounds, non-mesomorphic as well as mesomorphic, were used. These are listed in table 2.4.

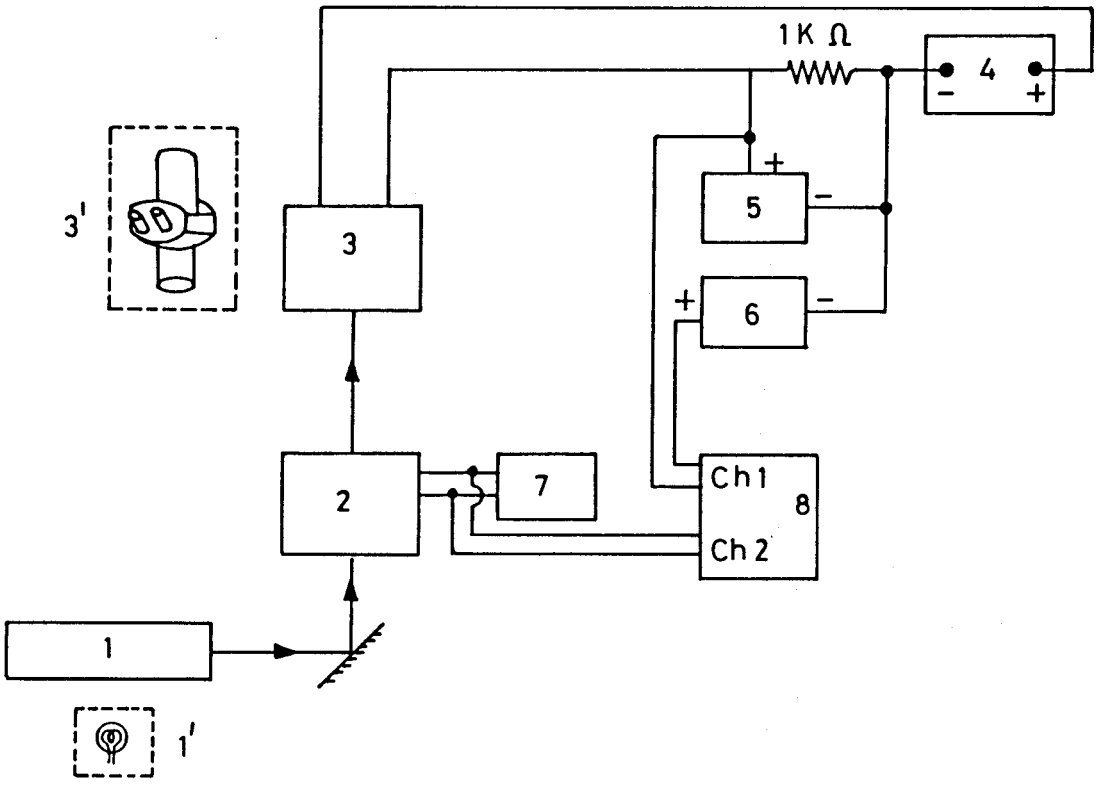

Figure 2.15

Schematic diaglram of the experimental set up used for the high pressure experiments.

1. He-Ne laser, 2. High pressure optical cell, 3. Photo detectoz, 4. Photo detector bias power supply, 5. Multimeter for measuring intensity in terms of voltage, 6. DC standard source used for voltage off set, 7. Multimetet for measuring thermocouple output, 8. Multichannel recorder.

Instruments indicated by plrimed numbers are used for microscopic observations.

Table 2.4

Materials used for the temperature calibration

Sl. No.	Compound	Abbreviation
1	trans-4-alkyl-4'-cyanocyclohexyl-cyclohexane	C - CH_n (n = 2,4)
2	4-Nitrophenyl-4'-n-octyloxybenzoate	NPOOB
3	4-Heptyloxy-4'-decyloxybenzoate	7OPDOB
4	n-p-cyanobenzylidene-p-nonylaniline	CBNA
5	4,4'-di-n-heptyloxyazoxybenzene	HOAB
6	4,4'-di-methoxyazoxybenzene (p-azoxyanisole)	PAA
7	p-Azoxyphenetole	PAP

a) Heating mode

The transition temperatures of the materials were measured on the heating mode using a polarizing microscope fitted with a programmable hot stage (Mettler FP82/FP800) are listed in table 2.5. The plot of these temperatures against the transition temperatures of the same materials as determined 'in-situ' in the high pressure cell using the optical transmission technique is shown in Fig. 2.16. The data were fitted to a straight line using a linear least square program. The values of slope and intercept thus obtained are 1.000 and 1.571°C respectively.

b) Cooling mode

Since crystallization temperature depends on the experimental conditions, it was found necessary to use only mesophase-mesophase transitions, which are reproducible in the cooling mode, for the purpose of calibration. The compounds used are listed in Table 2.6 along with the transition temperatures as determined using Mettler hot-stage. The plot of these temperatures against the temperature measured 'in-situ' in the high pressure cell is shown in Fig. 2.17. The values of the constants of this linear plot are 0.985 and -0.269°C.

c) Pressure Calibration of the Cell

In order to ascertain that the pressure experienced by

Table 2.5

Materials used for the temperature calibration of the high pressure cell (heating mode) and their transition temperatures

Sl No	Substance	Transition	Actual temp. (°C) by Mettler	Observed temp. (°C) (by pressure cell)
1	C - CH_2	Nematic–Isotropic	48.5	57.1
2	Azobenzol	Solid - Isotropic	67.9	69.2
3	NPOOB	Nematic–Isotropic	66.2	69.5
4	C - CH_4	Nematic - Isotropic	79.2	80.6
5	Benzil	Solid–Isotropic	94.7	96.4
6	7OPDOB	Solid - Smectic C	69.7	71.1
		Smectic A –Nematic	84.1	85.1
		Nematic - Isotropic	87.8	88.8
7	CBNA	Solid - Smectic A	72.0	73.3
		Smectic A - Nematic	99.3	100.2
		Nematic - Isotropic	105.0	106.1
8	HOAB	Solid–Smectic C	74.4	75.8
		Smectic C - Nematic	94.6	95.5
		Nematic - Isotropic	123.8	125.7
9	PAA	Solid - Nematic	118.0	119.9
		Nematic–Isotropic	135.2	137.1
10	PAP	Solid–Nematic	140.0	141.6
		Nematic– Isotropic	165.2	167.4

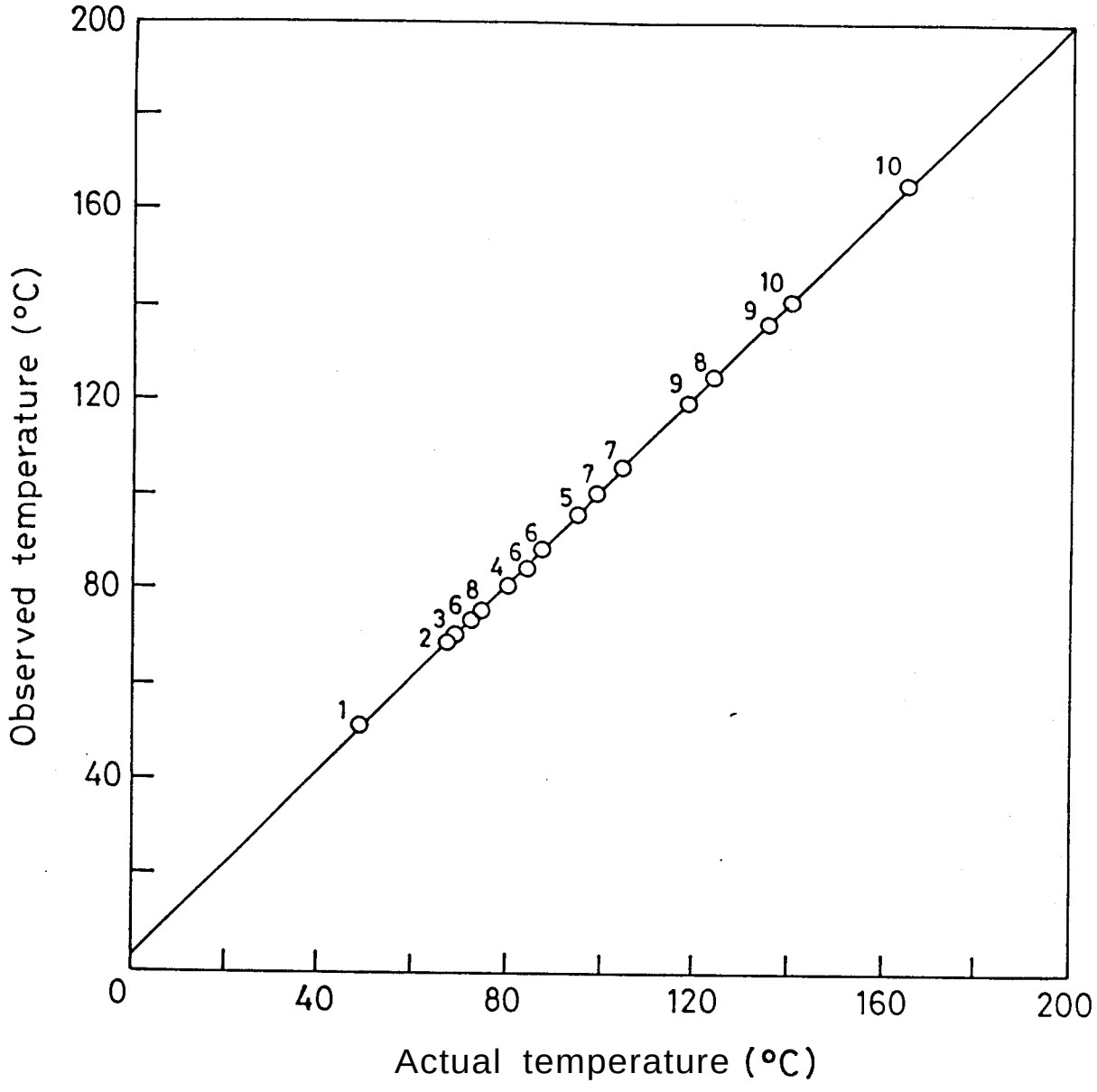

Figure 2.16

Temperature calibiation cuive on heating mode. The data points marked correspond to those given in Table 2.5.

Table 2.6

Temperature calibration of the high pressure cell during cooling mode: Materials used and their transition temperatures

Sl. No.	Substance	Transition	Actual temp.(°C) by Mettler	Observed temp. (°C) by pressure cell
1	C - CH_2	Isotropic– Nematic	48.40	46.10
2	NPOOB	Isotropic–Nematic	66.20	65.80
		Nematic - Smectic A	60.10	59.30
3	C - CH_4	Isotropic - Nematic	79.00	77.80
4	7OPDOB	Isotropic –Nematic	87.60	86.20
		Nematic - Smectic A	84.00	82.70
5	CBNA	Isotropic –Nematic	104.90	103.70
		Nematic–Smectic A	99.10	97.20
6	HOAB	Isotropic –Nematic	123.60	122.20
		Nematic–Smectic C	94.30	91.90
7	PAA	Isotropic - Nematic	135.00	132.40
8	PAP	Isotropic–Nematic	165.00	161.90

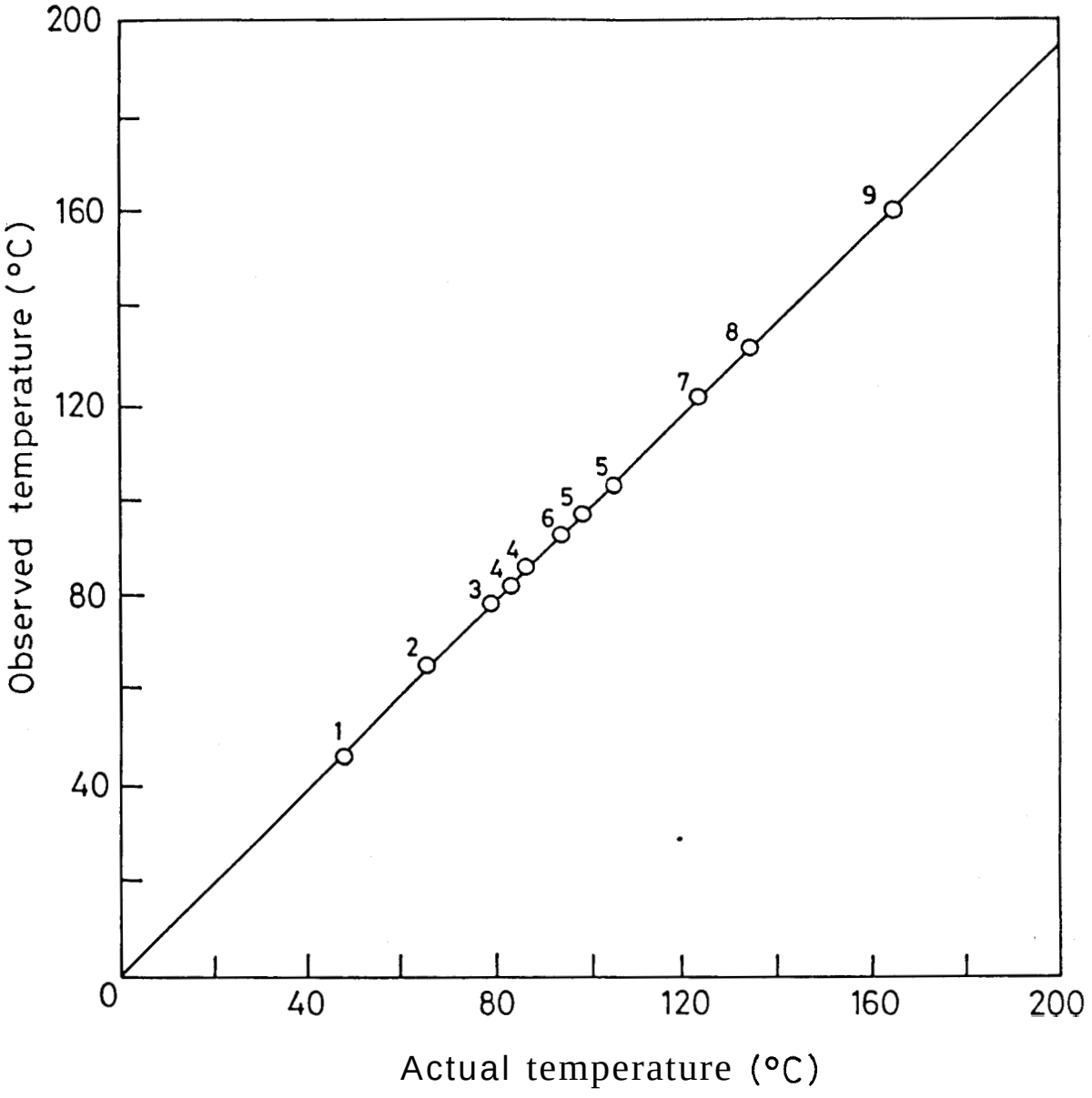

Figure 2.17

Temperature calibration curve during cooling. The data points marked correspond to those listed in Table 2.6.

the sample is the same as the line pressure read in the gauge, we conducted calibration experiments using p-azoxyanisole (PAA), perhaps the most widely studied liquid crystal under pressure.[11-20] The nematic-isotropic transition was used for the purpose. The experiments were conducted on both increasing and decreasing pressure cycle and it was found that the transition temperature at any pressure was independent of the pressure cycling. This showed that the sample in the cell was experiencing hydrostatic pressure. The accuracy of pressure measurements was ±1.5 bar.

REFERENCES

I P.E.Cladis and D.Guillon (Private communications)

2 A.J.Leadbetter, J.C.Frost, J.P.Gaughan, G.W.Gray and A.Mosley J. de Phys., 40, 375 (1979)

3 F.Hardouin, A.M.Levelut, J.J.Benattar and G.Sigaud, Solid State Commun., 33, 337 (1980)

4 S.Chandrasekhar and R.Shashidhar, "Advances in Liquid Crystals", Vol. 4, Ed. G.H.Brown (Academic Press, 1979), p. 83

5 G.A.Hullett, Z. Phys. Chern., 28, 629 (1899); J. Robberecht, Bull. Soc. Chim. Belg., 47, 597 (1938)

6 P.H.Keyes, H.T.Weston and W.B.Daniels, Phys. Rev. Lett., 31, 628 (1973)

7 P.E.Cladis, R.K.Bogardus, W.B.Daniels and G.N.Taylor, Phys. Rev. Lett., 39, 720 (1977)

8 A.N.Kalkura, R.Shashidhar and M.Subramanya Raj Urs, J. de Phys., **44**, 51 (1983); A.N.Kalkura, "High Pressure Optical Studies of Liquid Crystals", Ph. D. Thesis, University of Mysore, 1982

9 S.Krishna Prasad, "High Pressure Studies of Liquid Crystalline Transitions", Ph. D. Thesis, University of Mysore, 1985.

10 R.Shashidhar, B.R.Ratna and S.Krishna Prasad, Phys. Rev. Lett., 53, 2141 (1984)

11 G.A.Hulett, Z. Phys. Chem., 28, 629 (1899)

12 N.A.Puschin and I.W.Grebenschtschikow, Z. Phys. Chem., 57, 270 (1926)

13 J.Robberecht, Bull. Soc. Chim. Belg., 47, 597 (1938)

14 N.A.Tikhomirova, L.K.Vistin and V.N.Nosov, Sov. Phys. Crystallogr. (Engl. Trans.), 17, 878 (1973).

15 S.Chandrasekhar, S.Ramaseshan, A.S.Reshamwala, B.K.Sadashiva, R.Shashidhar and V.Surendranath, Proc. Int. Liq. Cryst. Conf., Bangalore, 1973 - Pramana, Suppl. 1, 117 (1975)

16 W.Klement and L.H.Cohen, Mol. Cryst. Liq. Cryst., 27, 359 (1974)

17 W.Spratte and G.M.Schneider, Ber. Bunsenges. Phys. Chem., 80, 886 (1976)

18 B.Deloche, B.Cabane and D.Jerome, Mol. Cryst. Liq. Cryst., 15, 197 (1971)

19 V.Ya.Baskakov, V.K.Semenchenko and N.A.Nedostup, Sov. Phys. Crystallogr. (Engl. Trans.), 19, 112 (1974); V.Ya.Baskakov, V.K.Semenchenko and V.M.Byankin, Sov. Phys. JETP (Engl. Trans.), 39, 383 (1974)

20 S.M.Stishov, V.A.Ivanov and V.N.Kachinskii, JETP Lett. (Engl. Trans.), 24, 297 (1977).